# Upregulation of G Protein-Coupled Estrogen Receptor by Chrysin-Nanoparticles Inhibits Tumor Proliferation and Metastasis in Triple Negative Breast Cancer Xenograft Model

Kyoung Mee Kim and Joohee Jung*

College of Pharmacy, Duksung Women's University, Seoul, South Korea

Triple-negative breast cancer (TNBC) is associated with a high mortality rate among women globally. TNBC shows a high rate of recurrence and distant metastasis. Particularly, the chemotherapy is limited because hormone therapy of breast cancer is ineffective. Thus, an effective chemotherapeutic agent is needed for tumor suppression. Chrysin-nanoparticles (chrysin-NPs) were investigated for their inhibitory effect on a MDA-MB-231-derived xenograft model. To gain insight into the underlying mechanisms, we conducted human matrix metalloproteinase (MMP) array, western blot, and immunohistochemistry analysis. Furthermore, *in vivo* imaging was used to monitor the chemotherapeutic efficacy of chrysin-NPs in a metastasis mouse model. Chrysin-NPs significantly inhibited the proliferation of MDA-MB-231 cells *via* the PI3K/JNK pathway and induced cell death through the p53-apoptosis pathway, leading to delayed MDA-MB-231-derived tumor growth. Interestingly, chrysin-NPs significantly induced G protein-coupled estrogen receptor (GPER) expression, which suppresses MMPs and NF-κB expression. Chrysin-NPs acted as effective metastasis inhibitors. Our results suggest that chrysin-NPs may be used as an effective adjuvant formulation to inhibit TNBC progression.

Keywords: chrysin-nanoparticle, triple-negative breast cancer, metastasis, tumor progression, G protein-coupled estrogen receptor

## INTRODUCTION

Breast cancer is a leading cause of deaths in woman worldwide (1, 2). Breast cancer is divided into four different subtypes; luminal A (estrogen receptor (ER) and progesterone receptor (PR) positive, human epidermal receptor 2 (HER2) negative and low Ki-67 level), luminal B (ER and PR positive, HER2 positive or negative and high Ki-67 level), HER2 enrich (ER and PR negative), and triple negative (ER, PR, and HER2 negative) (3, 4). The therapeutic modalities for triple-negative breast cancer (TNBC) are limited to surgery or conventional chemotherapy as TNBC patients will not respond to endocrine therapy or receptor targeting treatments (5). TNBC accounts for 15% of all cases of breast carcinoma (6), has the poorest overall survival of all breast cancer subtypes (7), and

has the highest rates of epithelial-to-mesenchymal transition (EMT) metastasis, possibly resulting from the remarkable phenotypic similarity between TNBC cells and mammary stem cells (8).

Therefore, development of targeted therapies for TNBC is urgently needed. The course of tumor metastasis entails a series of stages that lead to the formation of secondary tumors in distant organs (9). The process of invasion is instigated as the original tumor cells pass through the basement membrane and extracellular matrix, journey through the circulatory system, and attach at a new location to proliferate and produce secondary tumors (10, 11). Resultantly, research efforts focused on identifying and understanding the mechanisms concerned in tumor cell invasion may lead to the development of novel approaches to inhibit tumor progression in TNBC patients. The key enzymes responsible for ECM breakdown are matrix metalloproteinases (MMPs), a family of zinc- and calcium-dependent endopeptidases involved in the regulation of cell growth, migration, angiogenesis and invasion (11–13). The role of MMPs in a variety of cancers has been reviewed elsewhere (14, 15). In breast cancer, the expression levels of MMPs were reported to be higher than in normal breast tissues (16, 17). For instance, MMP-1,−2,−7,−9,−10,−11,−13,−14, and−15 were documented for their contribution to breast cancer proliferation and metastasis (18–21). Previous studies have reported that the G protein-coupled estrogen receptor-1 (GPER, formerly known as GPR30) was associated with disease progression in cancer patients (22). A wide number of natural and synthetic compounds, including estrogens and anti-estrogens, elicit stimulatory effects in breast cancer through GPER upregulation and activation (23). Estrogen signaling and ERα are well-documented for their contribution to the progression of ER-positive breast cancers (24). In TNBC patients who lack the expression of ER, stimulation by estrogen or/and anti-estrogen is mediated via GPER (24–26), supporting the contributory role of GPER in TNBC disease progression (26). Other authors have also reported that GPER is involved in the development and/or proliferation of renal (27), endometrial (28, 29), and ovarian cancers (30, 31).

Chrysin, also called 5,7-dihydroxyflavone, is a flavone found in the clock flower and in honeycomb (32). It has various physiological activities including anti-inflammatory, antioxidant, hypoglycemic and anti-aromatase activity (32). The compound was reported to inhibit the proliferation of non-small cell lung cancer cells (33, 34). In another study, it was confirmed that invasion and migration of TNBC MDA-MB-231 cells were reduced in the presence of low concentrations of chrysin (7). However, chrysin is difficult to apply to *in vivo* system because it is insoluble in water. Thus, chrysin is effective, but its reports are limited (35, 36). In order to overcome the disadvantages (solubility and degradation), many researchers are studying to improve the efficacy and effectiveness of the drug by using a drug delivery system (37, 38). Among many drug delivery systems, polymers that synthesize biodegradable polyesters have been applied for many years (39–41), nanoparticles composed of hydrophobic poly (ε-caprolactone) (PCL) and hydrophilic poly(ethylene glycol) (PEG) among several polymers (42, 43)

have been reported to be good potential carriers for anti-cancer agents (39, 44). PCL is a biodegradable, biocompatible, hydrophobic and non-toxic thermoplastic polyester (45). PEG is a common constituent for the hydrophilic outer shell and is known to reduce the adhesion of plasma proteins, solubility in water and organic solvents, stabilization of particles, and lack of toxicity (46, 47). In addition, it has been reported that polymeric nanoparticles with hydrophilic PEG outer shell can increase the circulation time of the hydrophobic anticancer agents in the body and prevent recognition by macrophages of the reticuloendothelial system (RES) after intravenous administration (47, 48). Additionally, PCL-PEG nanoparticles (without drug) were non-toxic in the liver and kidney of mice (49). Several researches reported that polymer could improve the bioavailability of chrysin (33, 50).

The aim of our study was to determine whether chrysin-nanoparticles (chrysin-NPs) may be used as an effective adjuvant formulation to inhibit the progression and metastasis of TNBC using a xenograft model.

## MATERIALS AND METHODS

### Preparation of Chrysin-NPs

Chrysin-NPs were produced as previously described, with minor modifications (**Figure 1**) (33). In brief, chrysin and polyethylene glycol-β-polycaprolactone copolymer (mPEG-PCL, PolySciTech, West Lafayette, IN, USA) were mixed at a ratio 1: 10 (w/w) in dichloromethane (DCM): methanol (1.5:1 v/v, Duksan reagent, Gyeonggi-do, Korea) solution. The mixture was then homogenized for 1 min and a solution of 1% polyvinyl alcohol was added to create an emulsion. Chrysin-NPs micelles were obtained upon evaporation. Chrysin-loading efficiencies were calculated as a previous report (33). Chrysin-NPs were prepared when it used. The average of encapsulated efficiency was 61.1% in chrysin-NPs.

### Cell Culture

MDA-MB-231 and MDA-MB-231_luc cells (luciferase-expressing cells, kindly provided from Prof. Moon, Duksung Women's University) were maintained in RPMI-1640 medium (GenDEPOT, Barker, TX, USA) containing 10% fetal bovine serum (YOUNGINFRONTIER, Seoul, Korea) and 1% penicillin/streptomycin (GenDEPOT) in a 5% $CO_2$ humidified atmosphere at 37°C.

### MTT Assay

MDA-MB-231 cells (5,000 cells/well) were seeded in 96-well plates and incubated for 24 h. Chrysin (Sigma-Aldrich, St Louis, MO, USA), NP or chrysin-NPs were then added for a 48 h-incubation period. G-1 and G-15 (Cayman Chemical, Michigan, USA) were added for a 24 and 48 h-incubation period. MTT (Sigma-Aldrich) was added to the media for a further 3 h, and the supernatant was gently removed and discarded. DMSO (Sigma-Aldrich) was added and absorbance (560 nm) was determined using a microplate reader (Infinite M200 PRO; Tecan Inc., Grödig, Austria). The data were represented a mean ± standard deviation (SD, n = 4).

**FIGURE 1 |** Production flowchart of chrysin-loaded nanoparticles.
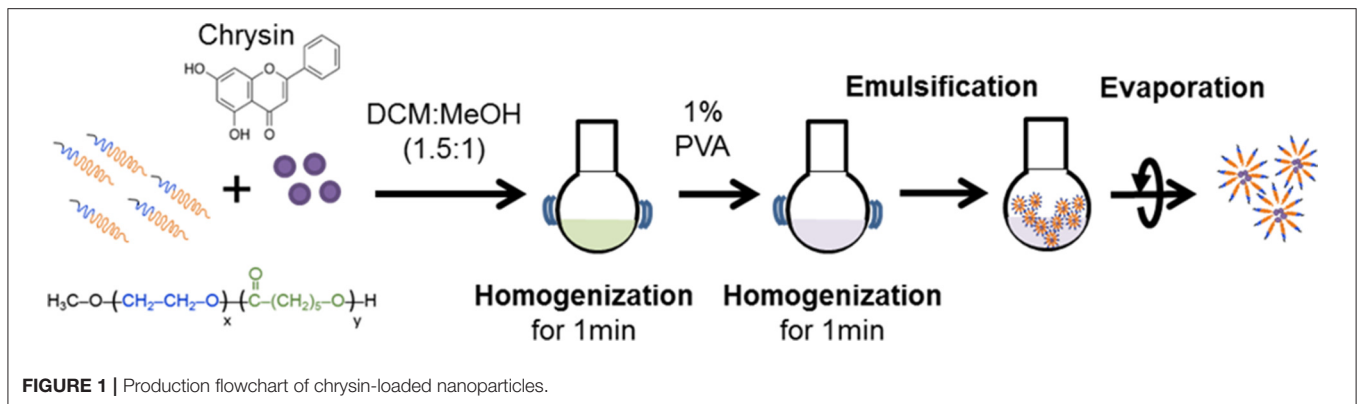
## Experimental *in vivo* Study

All animal experiments were approved by the Institutional Animal Care and Use Committee of Duksung Women's University in accordance with the guidelines for the care and use of laboratory animals. Five-weeks-old female Balb/c nude mice were obtained from JUNGAH BIO (Gyeonggi, Korea). Healthy mice were left to acclimatize for 1 week prior to any procedural work. The conditions in the laboratory were 20°C, 50% humidity, and a 12/12-h light/dark cycle. Diet was provided with drinking water *ad-libitum*.

## *In vivo* Tumor Growth Monitoring

MDA-MB-231 cells ($5 \times 10^6$ cells/mouse) were orthotopically implanted into the mammary fat pads of mice. When MDA-MB-231-derived tumor reached at volume of 150–200 mm$^3$, mice were randomly divided into 2 groups ($n = 6$/group). Tumor sizes were measured three times per week. Tumor volumes were calculated using the following equation:

Tumor volume (mm$^3$) = (Length × Width$^2$) × 0.5

The data were represented as mean ± standard deviation (*SD*).

## Luminescence Measurement Using *in vivo* Imaging

MDA-MB-231_luc cells ($1 \times 10^5$ cells/mice) were intravenously injected into the tail vein of NGRA mice (5-weeks-old, female). To track tumor cell movement, 100 μL of D-luciferin (XenoLightTM D-luciferin potassium salt, PerkinElmer, EU) was intraperitoneally injected two times per week to NGRA mice bearing MDA-MB-231_luc cells. Mice were anesthetized with isoflurane (TerrellTM, Piramal, PA, USA) and their luminescence was quantified within 10 min of the injection using an *in vivo* imaging system (VISQUETM *in vivo* Elite, Vieworks, Gyeonggi-do, Korea). When luminescence was detected, mice were randomly divided into two groups ($n = 3$/group).

## Administration of Chrysin-NPs

The mouse control group was injected with saline and the treated group was intravenously injected with chrysin-NPs (10 mg/kg) three times per week for 20 days. Mouse body weights were recorded three times per week.

## Western Blot Analysis

Tumor tissues were homogenized in a radioimmunoprecipitation assay (RIPA) buffer (GenDEPOT) containing a protease and phosphatase inhibitor cocktail (GenDEPOT). The extracted proteins were quantified using a bicinchoninic acid (BCA) assay (Thermo Scientific, Waltham, MA, USA). Proteins were then separated using 12% SDS-polyacrylamide gel electrophoresis (SDS-PAGE) and transferred to polyvinylidene fluoride (PVDF) membranes (Millipore, Darmstadt, Germany). Membranes were blocked with 5% skimmed milk in tris-buffered saline supplemented with polysorbate 20 (TBST) (50 mM Tris-HCl pH 7.4, 150 mM NaCl, 0.1% Tween20), washed and incubated with anti-p-JNK antibody (sc-12882, Santa Cruz Biotechnology, Texas, USA, 1:1,000), anti-JNK antibody (sc-571, Santa Cruz Biotechnology, 1:1,000), anti-Akt antibody (H-136, sc-8312, Santa Cruz Biotechnology, 1:1000), anti-p-Akt (C400, Cell signaling technology, MA, USA, 1:1000), anti-GSK-3α/β antibody (sc-7291, Santa Cruz Biotechnology, 1:1000), anti-NK-κB antibody (MAB3026, Millipore, Darmstadt, Germany, 1:1000), anti-MMP-10 antibody (sc-80197, Santa Cruz Biotechnology, 1:1,000), anti-MMP-2 antibody (MAB13405, Millipore, 1:1000), anti-PI3K antibody (C73F8, Cell signaling technology, 1:1000), anti-GPER antibody (ab188999, Abcam, USA, 1:1000) or anti-β-actin antibody (A4331, Sigma Aldrich, 1:5,000) at 4°C, overnight. The membrane was incubated with a secondary antibody (1:3,000) at room temperature for 3 h. Blots were visualized using enhanced chemiluminescent (ECL) solution and observed using the ChemiDocTM imager (FluorChemE, Germany). Images of western blots were quantified using Image J software.

## Human Mmatrix Metalloproteinase Antibody Array

MMP-related proteins were detected using a human MMP array kit (RayBiotech, USA). The extracted tumor tissues were lysed using a RIPA buffer (GenDEPOT) containing a protease and phosphatase inhibitor cocktail (GenDEPOT). The resulting lysate was applied to the membrane array kit and incubated overnight at 4°C. After several washings, the membrane was incubated with HRP-Streptavidin for 2 h at room temperature, washed and further incubated with the kit detection buffer for

2 min at room temperature. MMP-related protein expression was observed using the ChemiDocTM imager.

## Tissue Preparation

Tumor tissues were isolated and embedded into optical cutting temperature (OCT) compound (Leica, Nussloch, Germany) or paraffin. Frozen or paraffin blocks were sectioned into 5 μm slices.

## TUNEL Assay

TUNEL assay was performed as previously described (33). Sections were hydrated with 100, 90, and 70% ethanol, bathed in 3% $H_2O_2$/distilled water (DW), washed with DW, and then incubated in DW at 60°C for 1 h. The sections were subsequently cooled to room temperature for 1 h, treated with terminal deoxynucleotidyl transferase (TdT) labeling buffer, and then incubated in TdT (Sigma)/biotinylated deoxyuridine (Roche Diagnostics, Mannheim, Germany) for 1 h at 37°C in a humidified chamber. The reaction was stopped using terminating buffer, and slides were washed with DW. The tissue sections were then blocked with 2% bovine serum albumin (BSA; bioWORLD, Dublin, OH, USA) in PBS, washed and incubated with the ABC complex also diluted in PBS. A final wash was carried out using 0.05 M Tris buffer, and color development with DAB substrate (Vector laboratories, Inc., Burlingame, CA, USA). Results were examined under a microscope (Leica). Images of tissues ($n = 5$, each group) were quantified using Image J software and plotted as percent of stained area.

## Immunohistochemistry

Immunohistochemical staining was performed as previously described (33). Tissue sections were incubated with anti-Ki-67 antibody (ab16667, Abcam, 1:100) and the expression of Ki-67 was visualized using a DAB peroxidase substrate kit (Vector laboratories). Cell nuclei were visualized using hematoxylin-based counterstain solution (Sigma-Aldrich).

## Statistical Analysis

All data were analyzed using Prism7 (GraphPad Software Inc., San Diego, CA, USA) using Student's $t$-test or ANOVA test. Differences were considered statistically significant when $p$-value was inferior to 0.05.

## RESULTS

### Chrysin-NPs Inhibit Metastasis-Related Signaling and Induce Cell Death in MDA-MB-231 Cells

The anti-cancer properties of chrysin-NPs were investigated in MDA-MB-231 TNBC-like cells using an MTT assay (**Figure 2A**). Our results showed that chrysin-NPs inhibited cell viability in a dose-dependent manner, in a similar manner to chrysin itself. No change in cell viability was detected in the NP-vehicle control wells. These observations suggest that, when delivered in a nanoparticulate format, chrysin maintained its anti-cancer properties *in vitro*. Upon western blot analysis of the expression levels of molecules known to be involved in cancer progression

(**Figure 2B**), we found that PI3K and NF-κB levels were found to be lower upon treatment with chrysin-NPs. Similarly, the expression levels of MMP-10 and MMP-2, which are known to play a role in invasion and metastasis, were also in decline.

### Chrysin-NPs Delay Tumor Growth Through Apoptosis

To evaluate the chemotherapeutic efficacy of chrysin-NPs, tumor growth was compared between control and chrysin-NP-treated mice. A chrysin only treated group was omitted in this study on the basis that in a previous study, chrysin-NPs were shown to be injectable and effective at preserving its biological activities *in vivo* (33). Upon repeated administration of chrysin-NPs, a significant growth delay was observed in MDA-MB-231-derived tumors (**Figure 3A**). Additionally, a decrease in tumor weight was detected in mice treated with chrysin-NPs, but the data were not significantly different due to the large difference in individual data (**Figure 3B**). Similarly, the expression level of Ki-67, a proliferation marker, declined in mice that were administered with chrysin -NPs compared to control mice (**Figure 3C**). The tumor tissues treated with chrysin-NPs presented the morphological hallmarks of apoptosis (**Figure 3D**, black arrow). Apoptotic cells (stained area) were quantified (**Figure 3D**, graph). The tumor tissues treated with chrysin-NPs significantly increased apoptosis. Altogether, our results indicate that chrysin-NPs significantly repressed TNBC-derived tumor growth through inhibition of proliferation and induction of apoptosis.

### Chrysin-NPs Suppress Metastatic Signaling in MDA-MB-231-Derived Tumors

We previously showed (**Figure 2**) that chrysin-NPs exerted inhibitory effects on cancer progression *in vitro*. Here we sought to determine whether chrysin-NPs could exert any inhibition on the invasion mechanisms *in vivo*. The expression levels of MMPs were measured to evaluate invasion and migration in MDA-MB-231-derived tumor tissues. As shown in **Figure 4A**, the expression levels of MMP-1, 2, 3, 9, 10, and 13 declined in the tumor tissues isolated from mice treated with chrysin-NPs when compared with the control mice. On the other hand, the expression levels of MMP-8 (neutrophil collagenase) were on the rise upon treatment with chrysin-NPs, while expression of tissue inhibitor of metalloprotease (TIMP)-1 decreased. To gain insight into the mechanism of action of chrysin-NPs, we investigated the expression levels of markers of the PI3K/Akt pathway and GPER pathway on the basis of their reported contribution to MMPs expression, invasion, migration and metastasis (**Figure 4B**). Our results indicated a rise in the expression of PI3K and phospho-Akt (p-Akt), and a decrease in the expression of GSK-3β and NF-κB in tumors collected from mice treated with chrysin-NPs.

### Chrysin-NPs Inhibit Metastasis

We next sought to investigate the effect of chrysin-NPs on TNBC-derived metastasis *in vivo*. Chrysin-NPs treated mice were observed using an *in vivo* imaging system. While control mice showed a time-dependent increase in luminescence hence metastasis, the mice treated with chrysin-NPs showed
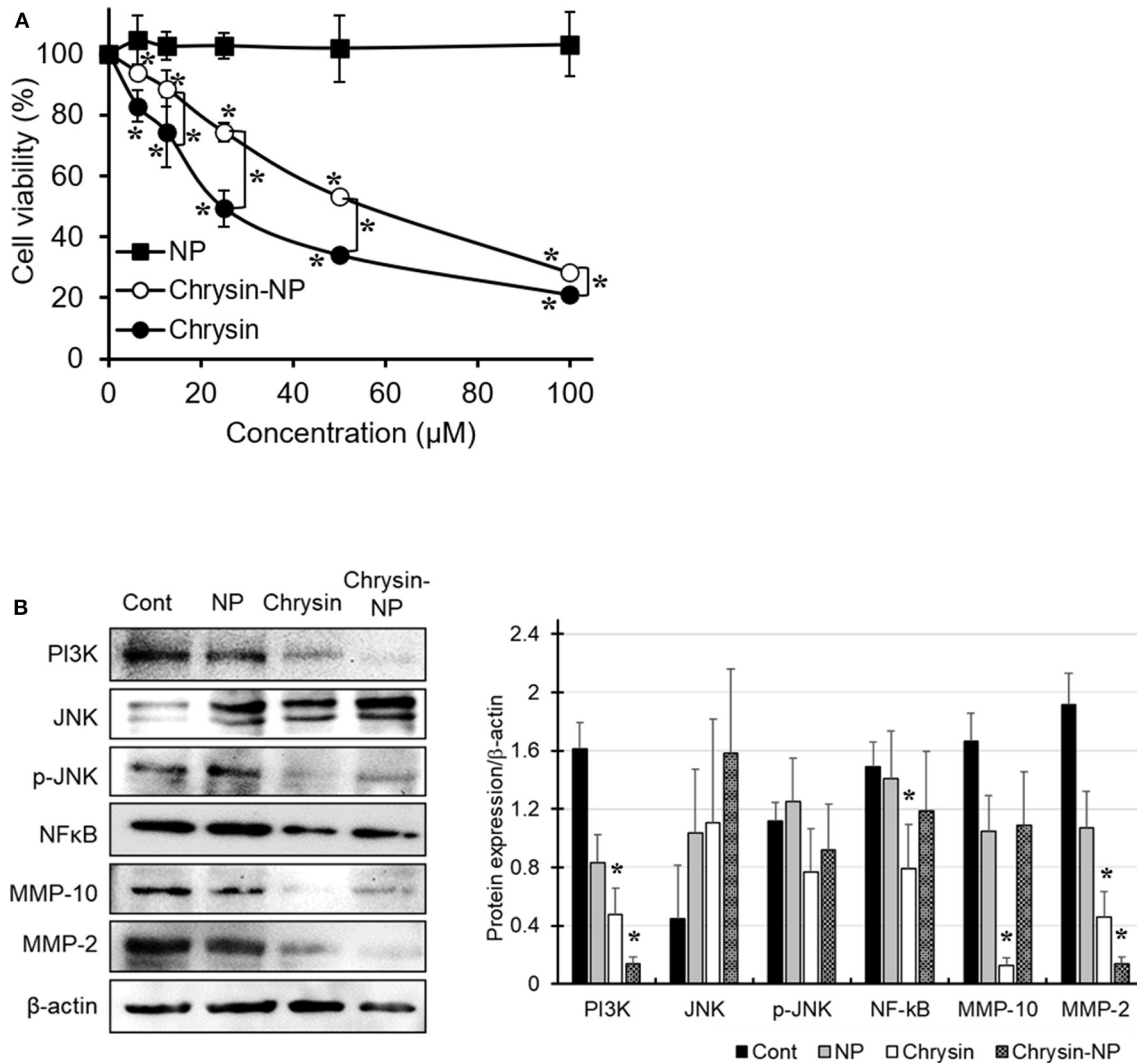
**FIGURE 2 |** Chrysin-NPs inhibit cell viability and PI3K/JNK signaling pathway. MDA-MB-231 cells were treated with chrysin or chrysin-NPs for 48 h. **(A)** Cell viability was assessed by MTT assay. Data were represented as mean ± S.D. ($n = 6$). *$p < 0.05$ (ANOVA). **(B)** The expression levels of PI3K/JNK signaling proteins were detected by western blot analysis. Data were represented as mean ± S.D. ($n = 3$). *$p < 0.05$ (ANOVA).

a significant lower incidence of metastasis (**Figures 5A,B**). In particular, the number and density of metastatic spots (**Figure 5C**, black arrows) observed in the liver tissues of control mice were higher than those observed in the liver tissues of chrysin-NPs-treated mice. The liver tissues of control mice showed tumor nests and loose blood vessels, while the liver tissues of chrysin-NPs treated mice didn't (**Figure 5D**).

## DISCUSSION

The aim of our study was to investigate the anti-cancer properties of chrysin encapsulated into mPEG-PCL nanoparticles. Our results showed that chrysin-NPs suppressed TNBC progression

via activation of the GPER signaling pathway *in vivo*. Chrysin-NPs induced apoptosis in MDA-MB-231-derived tumors (**Figure 3D**) and inhibited tumor growth in a xenograft model (**Figure 3A**). Furthermore, our data indicate that chrysin-NPs suppressed metastasis (**Figure 5**). Using these results, the proposed model was described for the inhibitory mechanism of tumor progression by chrysin-NPs in xenograft model (**Figure 6**).

In a previous study, we found that both chrysin-NPs and chrysin could delay tumor growth in a lung cancer xenograft model (33). Here, we showed that chrysin-NPs could inhibit the early stages of TNBC disease progression. Furthermore, chrysin-NPs lowered the expression levels of MMPs (**Figure 4A**). Several studies have reported that MMPs played an important role in cancer proliferation, angiogenesis, and metastasis in various
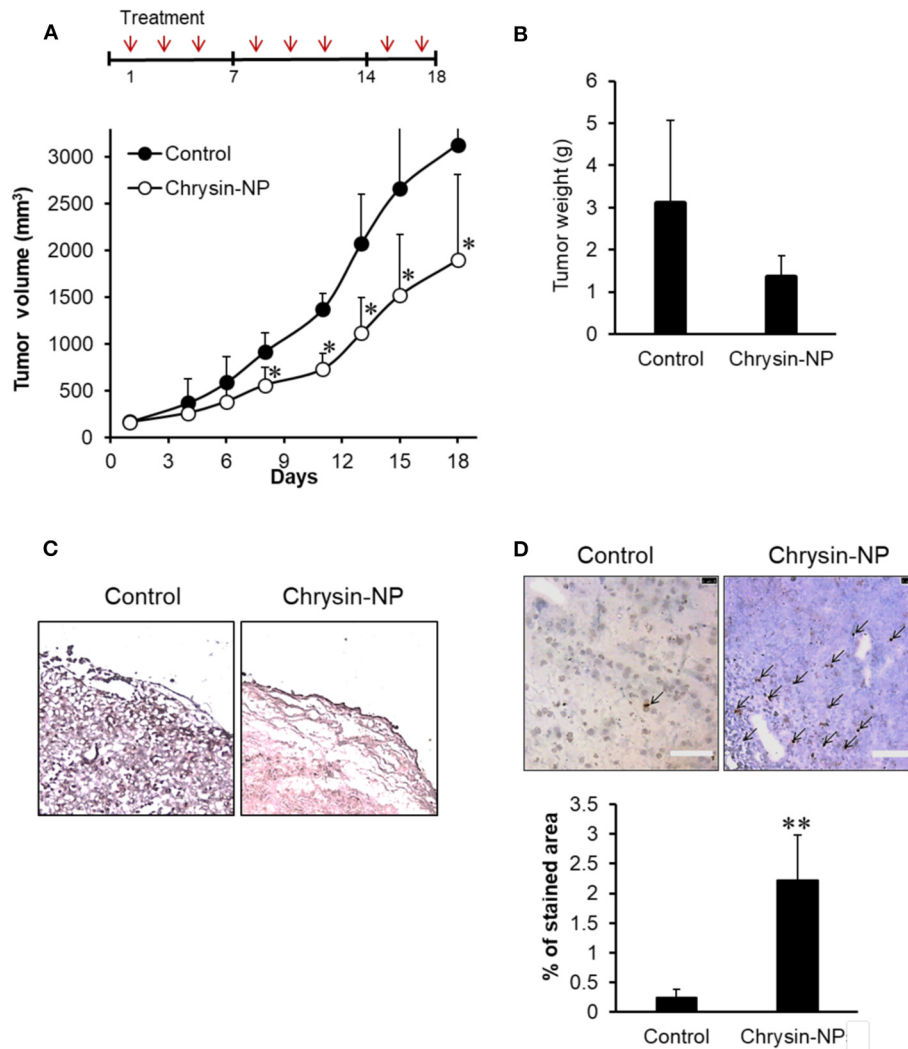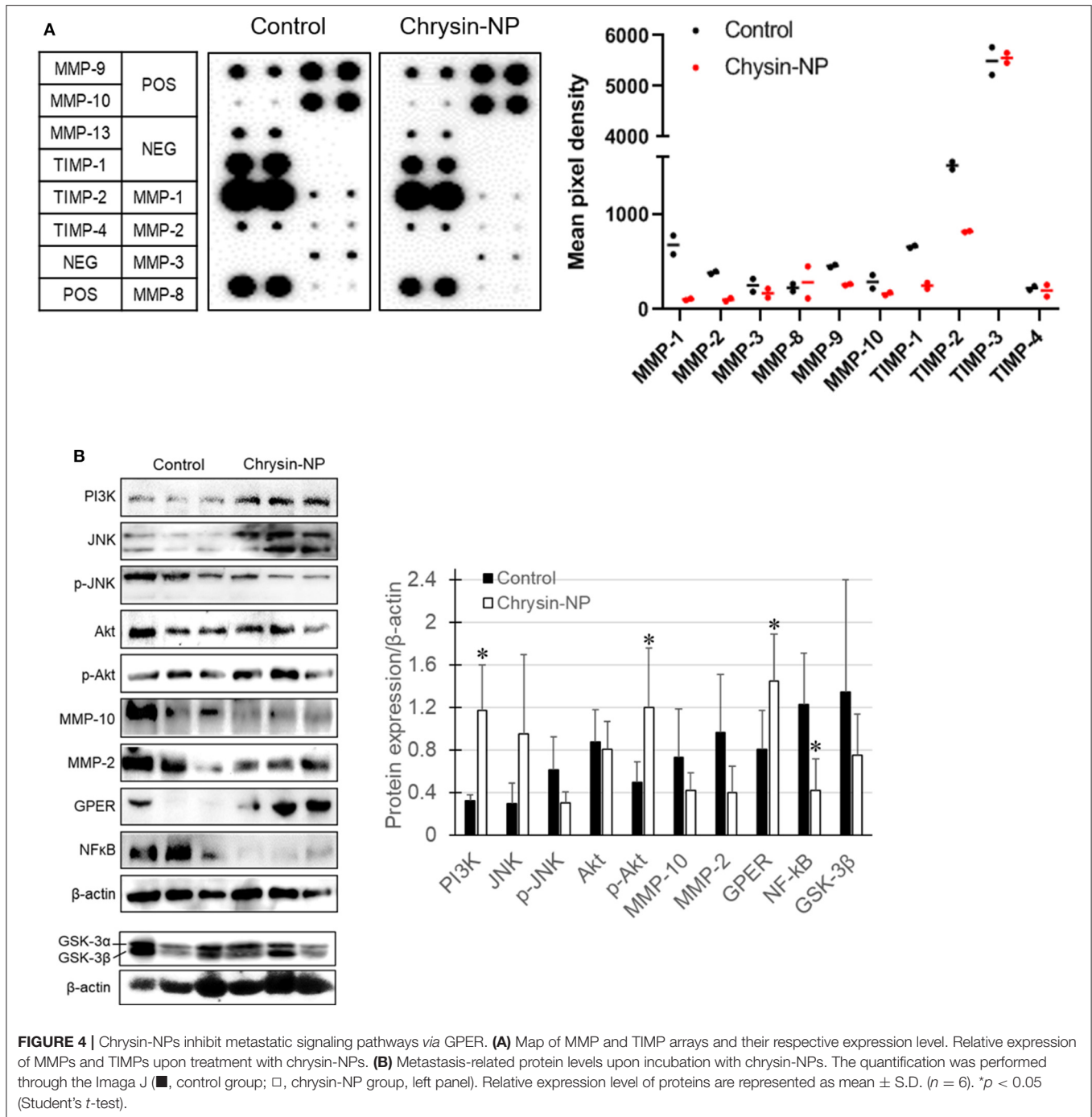
**FIGURE 3 |** Chrysin-NPs suppress tumor growth in MDA-MB-231-derived xenograft models. **(A)** Administration schedule of chrysin-NPs in mice. Chrysin-NPs (10 mg/kg) were administrated intravenously every other day, three times per week for 18 days. Growth curve of tumors in mice treated with chrysin-NPs. Data are represented as mean ± S.D. ($n = 6$). $^*p < 0.05$ (Student's $t$-test). **(B)** Comparison of tumor weights between sham-treated control and chrysin-NP treated group. Data are represented as mean ± S.D. ($n = 4$). **(C)** Expression of Ki-67 in MDA-MB-231-derived tumor tissues visualized by immunohistochemistry. Scale bar, 100 μm. **(D)** The brown spots (black arrows) denotes TUNEL-positive apoptotic cells. Scale bar, 100 μm. Apoptotic cells are quantified. Data are represented as mean ± S.D. ($n = 5$). $^{**}p < 0.005$ (Student's $t$-test).

cancers. Here chrysin-NPs inhibited the expression of MMP-1,−2,−3,−9,−10, and−13, while the expression of MMP-8 was higher in our MDA-MB-231-derived xenograft model than in the control group (**Figure 4A**). In particular, the expression levels of MMP-2 and−10 were consistently lower upon treatment with chrysin-NPs both *in vitro* and *in vivo* (**Figures 2**, **4**). These results are in line with previous studies (7). Down regulation of MMP-1,−2,−3,−9,−10, and−13 was associated with cancer progression and poor prognosis in breast cancer patients (16, 17, 51, 52). On the other hand, MMP-8 was shown to exert anti-proliferative and inhibitory activities on the spread of cancer cells to tissues, with a net inhibitory effect on metastasis (53). TIMP-1 was describe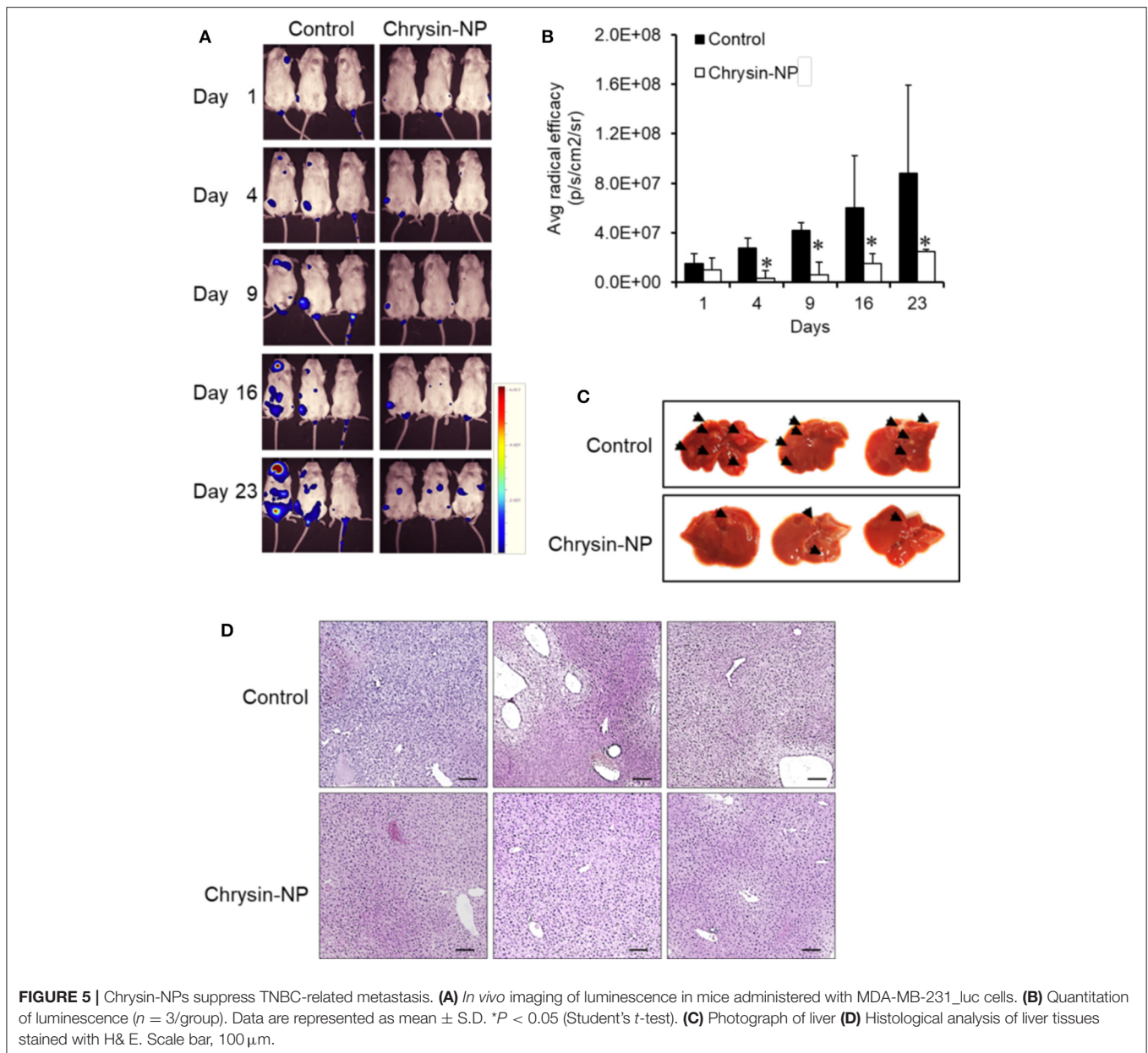d for its inhibitory activity on metalloproteinase, but there have been conflicting reports on its anti-apoptotic activity and its role in stimulating cell proliferation in breast cancer (10, 54). In the present study, the decreased expression of TIMP-1 upon treatment with chrysin-NPs was consistent with its anti-apoptotic activities. These results reinforce our observation that chrysin-NPs exert multiple suppressive effects on cancer progression *in vivo* through inhibition of TIMP-1, cell proliferation, and metastasis via downregulation of MMPs.

We next sought to elucidate the molecular mechanisms involved in MMPs signaling upon chrysin-NP treatment. The JNK signaling pathway is well-documented for its role in cancer progression and development. Activation of the JNK pathway was confirmed by western blot analysis of tumor tissue

**FIGURE 4 |** Chrysin-NPs inhibit metastatic signaling pathways *via* GPER. **(A)** Map of MMP and TIMP arrays and their respective expression level. Relative expression of MMPs and TIMPs upon treatment with chrysin-NPs. **(B)** Metastasis-related protein levels upon incubation with chrysin-NPs. The quantification was performed through the Imaga J (■, control group; □, chrysin-NP group, left panel). Relative expression level of proteins are represented as mean ± S.D. ($n = 6$). *$p < 0.05$ (Student's *t*-test).

homogenates: expression of total-JNK was not significant change upon treatment with chrysin-NPs while the expression of p-JNK was lower. Furthermore, expression levels of MMP-2, MMP-10, and NF-kB were lower in the chrysin-NPs-treated group as compared with the control group. Previous authors have reported that MMP-2 was regulated *via* PI3K and NF-kB pathway in breast cancer (55) and the inhibition of MMP-9 was associated with the inhibition of p-JNK (56). Our results also showed that the reduction of PI3K, p-JNK, and NF-kB by chrysin occurred the

inhibition of MMPs in MDA-MB-231 cells. However, chrysin-NPs induced PI3K/p-Akt expression level in MDA-MB-231-derived tumor tissues (**Figure 4B**). The result might be to cell-cell interaction, and crosstalk of cancer cell signaling and cells of tumor microenvironment (immune cells, fibroblast, stem cells). Chrysin-driven inhibition of MMP-10 was reported to be associated with the inhibition of p-Akt in breast cell lines (7). Our results also highlighted that chrysin-NPs induced higher *in vivo* activation of the PI3K/Akt signaling pathway compared

**FIGURE 5** | Chrysin-NPs suppress TNBC-related metastasis. **(A)** *In vivo* imaging of luminescence in mice administered with MDA-MB-231_luc cells. **(B)** Quantitation of luminescence ($n = 3$/group). Data are represented as mean ± S.D. *$P < 0.05$ (Student's $t$-test). **(C)** Photograph of liver **(D)** Histological analysis of liver tissues stained with H& E. Scale bar, 100 μm.

to chrysin alone (**Figure 4B**). Altogether, our results concur with the observation that chrysin-NPs may be used as an effective suppressor of cancer progression.

Next, we investigated the anti-metastatic efficacy of chrysin-NPs *in vivo*. As shown in **Figure 5**, the administration of chrysin-NPs led to significant inhibition of tumor cell metastasis. Downregulation of MMPs and TIMP-1 expressions upon treatment with chrysin-NPs was associated with lower levels of NF-kB. We also investigated the changes in expression of GPER upon treatment with chrysin-NPs. GPER is an alternate estrogen receptor with a structure distinct from the two canonical estrogen receptors, ERα and ERβ, and present multiple functions in a variety of tissues. Estrogen and/or anti-estrogen-induced effects mediated via GPER have been previously reported in TNBC.

GPER is also known to regulate estrogen signaling during the progression of TNBC, but the exact mechanisms remain unclear. Previous authors have reported that GPER activation by G-1 resulted in inhibition of metastasis and EMT via NF-κB (57), and suppression of tumor proliferation in breast cancer (29, 58, 59). GPER activation is also known to inhibit metastasis and proliferation in endometrial, ovarian, liver and adrenocortical cancers (28, 31, 60, 61). The activation of GPER, another target receptor in TNBC, was shown to inhibit cell migration and invasion (22). In contrast, other authors have reported that GPER activation could induce invasion and migration in kidney cancer, with a poor prognosis for the patients (24). Here, we showed that the administration of chrysin-NPs led to higher GPER expression levels in tumor tissues (**Figure 4B**), and lower expression levels of

**FIGURE 6 |** Proposed model for the mechanism of tumor suppression by Chrysin-NPs in TNBC cells.
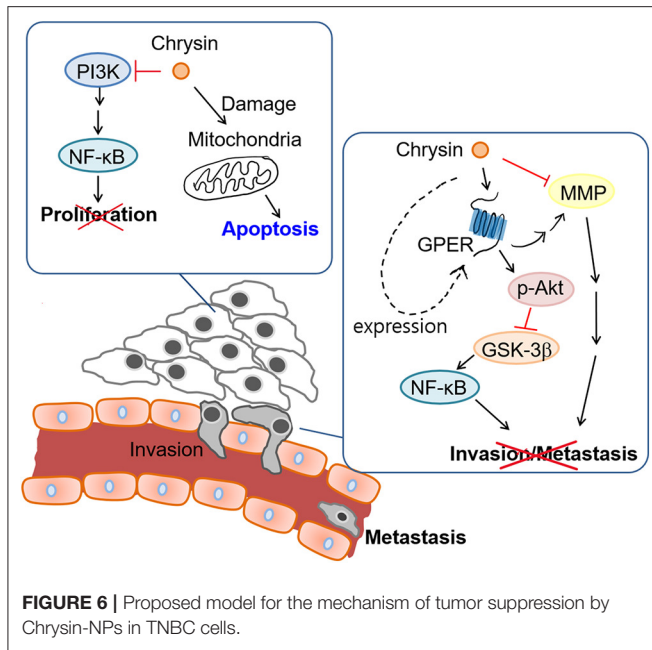
NF-κB, a signaling molecule downstream of GPER. As shown in **Figure 6** and **Supplementary Data**, PI3K/Akt signaling activated by GPER inhibited GSK-3β, an inhibitor of NK-kB (57, 62). The result suggests that chrysin could induce the GPER expression and suppress the metastasis of TNBC cells as a GPER agonist.

Our results showed that the loading of chrysin onto mPEG-PCL nanoparticles resulted in the enhancement of its anti-cancer properties. Most importantly, we found that chrysin-NPs activated a GPER-mediated NF-κB signaling pathway. These results strongly support that chrysin-NPs exert inhibitory effect on tumor growth and prevent metastasis. Hence our study supports the use of chrysin-NPs as a novel chemo-adjuvant for the treatment of TNBC patients.

## DATA AVAILABILITY STATEMENT

All datasets generated for this study are included in the article/**Supplementary Material**.

## ETHICS STATEMENT

The animal study was reviewed and approved by the Institutional Animal Care and Use Committee of Duksung Women's University.

## AUTHOR CONTRIBUTIONS

JJ: conceptualization, formal analysis, data curation, writing review, editing, visualization, supervision, project administration, and funding acquisition. KK: methodology, validation, and investigation. KK and JJ: writing original draft preparation. All authors have read and agreed to the published version of the manuscript.

## FUNDING

## ACKNOWLEDGMENTS

## SUPPLEMENTARY MATERIAL

The Supplementary Material for this article can be found online at: https://www.frontiersin.org/articles/10.3389/fendo.2020.560605/full#supplementary-material

## REFERENCES

1. Hong S, Won YJ, Park YR, Jung KW, Kong HJ, Lee ES, et al. Cancer statistics in korea: incidence, mortality, survival, and prevalence in 2017. *Cancer Res Treat.* (2020) 52:335–50. doi: 10.4143/crt.2020.206

2. Ghoncheh M, Pournamdar Z, Salehiniya H. Incidence and mortality and epidemiology of breast cancer in the world. *Asian Pac J Cancer Prev.* (2016) 17(Suppl.3):43–6. doi: 10.7314/APJCP.2016.17.S3.43

3. Dent R, Trudeau M, Pritchard KI, Hanna WM, Kahn HK, Sawka CA, et al. Triple-negative breast cancer: clinical features and patterns of recurrence. *Clin Cancer Res.* (2007) 13:4429–34. doi: 10.1158/1078-0432.CCR-06-3045

4. Sorlie T, Tibshirani R, Parker J, Hastie T, Marron JS, Nobel A, et al. Repeated observation of breast tumor subtypes in independent gene expression data sets. *Proc Natl Acad Sci USA.* (2003) 100:8418–23. doi: 10.1073/pnas.0932692100

5. Aydiner A, Derin D, Topuz E, Guney N, Saip P, Eralp Y, et al. MAPK overexpression is associated with anthracycline resistance and increased risk for recurrence in patients with triple-negative breast cancer. *Ann Oncol.* (2007) 19:669–74. doi: 10.1093/annonc/mdm522

6. deSantis C, Siegel R, Bandi P, Jemal A. Breast cancer statistics, 2011. *CA Cancer J Clin.* (2011) 61:409–18. doi: 10.3322/caac.20134

7. Yang B, Huang J, Xiang T, Yin X, Luo X, Huang J, et al. Chrysin inhibits metastatic potential of human triple-negative breast cancer cells by modulating matrix metalloproteinase-10, epithelial to mesenchymal transition, and PI3K/Akt signaling pathway. *J Appl Toxicol.* (2014) 34:105–12. doi: 10.1002/jat.2941

8. Foulkes WD, Smith IE, Reis-Filho JS. Triple-negative breast cancer. *N Engl J Med.* (2010) 363:1938–48. doi: 10.1056/NEJMra1001389

9. Lirdprapamongkol K, Sakurai H, Abdelhamed S, Yokoyama S, Maruyama T, Athikomkulchai S, et al. A flavonoid chrysin suppresses hypoxic survival and metastatic growth of mouse breast cancer cells. *Oncol Rep.* (2013) 30:2357–64. doi: 10.3892/or.2013.2667

10. Park SY, Kim YH, Kim Y, Lee SJ. Frondoside A has an anti-invasive effect by inhibiting TPA-induced MMP-9 activation via NF-kappaB and AP-1 signaling in human breast cancer cells. *Int J Oncol.* (2012) 41:933–40. doi: 10.3892/ijo.2012.1518

11. Stamenkovic I. Matrix metalloproteinases in tumor invasion and metastasis. *Semin Cancer Biol.* (2000) 10:415–33. doi: 10.1006/scbi.2000.0379

12. Bergers G, Coussens LM. Extrinsic regulators of epithelial tumor progression: metalloproteinases. *Curr Opin Genet Dev.* (2000) 10:120–7. doi: 10.1016/S0959-437X(99)00043-X

13. Tester AM, Waltham M, Oh SJ, Bae SN, Bills MM, Walker EC, et al. Pro-matrix metalloproteinase-2 transfection increases orthotopic primary growth and experimental metastasis of MDA-MB-231 human breast cancer cells in nude mice. *Cancer Res.* (2004) 64:652–8. doi: 10.1158/0008-5472.CAN-0384-2

14. Du X, Lin BC, Wang QR, Li H, Ingalla E, Tien J, et al. MMP-1 and Pro-MMP-10 as potential urinary pharmacodynamic biomarkers of FGFR3-targeted therapy in patients with bladder cancer. *Clin Cancer Res.* (2014) 20:6324–35. doi: 10.1158/1078-0432.CCR-13-3336

15. Zhang X, Yin P, Di D, Luo G, Zheng L, Wei J, et al. IL-6 regulates MMP-10 expression via JAK2/STAT3 signaling pathway in a human lung adenocarcinoma cell line. *Anticancer Res.* (2009) 29:4497–501.

16. Hegedus L, Cho H, Xie X, Eliceiri GL. Additional MDA-MB-231 breast cancer cell matrix metalloproteinases promote invasiveness. *J Cell Physiol.* (2008) 216:480–5. doi: 10.1002/jcp.21417

17. Benson CS, Babu SD, Radhakrishna S, Selvamurugan N, Ravi Sankar B. Expression of matrix metalloproteinases in human breast cancer tissues. *Dis Markers.* (2013) 34:395–405. doi: 10.1155/2013/420914

18. Pivetta E, Scapolan M, Pecolo M, Wassermann B, Abu-Rumeileh I, Balestreri L, et al. MMP-13 stimulates osteoclast differentiation and activation in tumour breast bone metastases. *Breast Cancer Res.* (2011) 13:R105. doi: 10.1186/bcr3047

19. Basset P, Bellocq JP, Wolf C, Stoll I, Hutin P, Limacher JM, et al. A novel metalloproteinase gene specifically expressed in stromal cells of breast carcinomas. *Nature.* (1990) 348:699–704. doi: 10.1038/348699a0

20. Sternlicht MD, Bergers G. Matrix metalloproteinases as emerging targets in anticancer therapy: status and prospects. *Emerg Therapeutic Targets.* (2000) 4:609–33. doi: 10.1517/14728222.4.5.609

21. Cathcart J, Pulkoski-Gross A, Cao J. Targeting matrix metalloproteinases in cancer: bringing new life to old ideas. *Genes Dis.* (2015) 2:26–34. doi: 10.1016/j.gendis.2014.12.002

22. Jung J. Role of G protein-coupled estrogen receptor in cancer progression. *Toxicol Res.* (2019) 35: 209–14. doi: 10.5487/TR.2019.35.3.209

23. Lappano R, Maggiolini M. G protein-coupled receptors: novel targets for drug discovery in cancer. *Nat Rev Drug Discov.* (2011) 10:47–60. doi: 10.1038/nrd3320

24. Liang S, Chen Z, Jiang G, Zhou Y, Liu Q, Su Q, et al. Activation of GPER suppresses migration and angiogenesis of triple negative breast cancer via inhibition of NF-kappaB/IL-6 signals. *Cancer Lett.* (2017) 386:12–23. doi: 10.1016/j.canlet.2016.11.003

25. Prossnitz ER, Barton M. The G-protein-coupled estrogen receptor GPER in health and disease. *Nat Rev Endocrinol.* (2011) 7:715–26. doi: 10.1038/nrendo.2011.122

26. Marjon NA, Hu C, Hathaway HJ, Prossnitz ER. G protein-coupled estrogen receptor regulates mammary tumorigenesis and metastasis. *Mol Cancer Res.* (2014) 12:1644–54. doi: 10.1158/1541-7786.MCR-14-0128-T

27. Liang S, Chen Z, Jiang G, Zhou Y, Liu Q, Su Q, et al. Corrigendum to "Activation of GPER suppresses migration and angiogenesis of triple negative breast cancer via inhibition of NF-kappaB/IL-6 signals" [Cancer Lett. 386 (2017) 12-23]. *Cancer Lett.* (2018) 414:310. doi: 10.1016/j.canlet.2017.10.025

28. Du GQ, Zhou L, Chen XY, Wan XP, He YY. The G protein-coupled receptor GPR30 mediates the proliferative and invasive effects induced by hydroxytamoxifen in endometrial cancer cells. *Biochem Biophys Res Commun.* (2012) 420:343–9. doi: 10.1016/j.bbrc.2012.02.161

29. Vivacqua A, Bonofiglio D, Recchia AG, Musti AM, Picard D, Ando S, et al. The G protein-coupled receptor GPR30 mediates the proliferative effects induced by 17beta-estradiol and hydroxytamoxifen in endometrial cancer cells. *Mol Endocrinol.* (2006) 20:631–46. doi: 10.1210/me.2005-0280

30. Ignatov T, Modl S, Thulig M, Weißenborn C, Treeck O, Ortmann O, et al. GPER-1 acts as a tumor suppressor in ovarian cancer. *J Ovarian Res.* (2013) 6:51. doi: 10.1186/1757-2215-6-51

31. Albanito L, Madeo A, Lappano R, Vivacqua A, Rago V, Carpino A, et al. G protein-coupled receptor 30 (GPR30) mediates gene expression changes and growth response to 17beta-estradiol and selective GPR30 ligand G-1 in ovarian cancer cells. *Cancer Res.* (2007) 67:1859–66. doi: 10.1158/0008-5472.CAN-06-2909

32. Jung J. Emerging utilization of chrysin using nanoscale modification. *J Nanomater.* (2016) 7:2016. doi: 10.1155/2016/2894089

33. Kim KM, Lim HK, Shim SH, Jung J. Improved chemotherapeutic efficacy of injectable chrysin encapsulated by copolymer nanoparticles. *Int J Nanomed.* (2017) 12:1917–25. doi: 10.2147/IJN.S132043

34. Lim HK, Kim KM, Jeong SY, Choi EK, Jung J. Chrysin increases the therapeutic efficacy of docetaxel and mitigates docetaxel-induced edema. *Integr Cancer Ther.* (2017) 16:496–504. doi: 10.1177/1534735416645184

35. Eatemadi A, Daraee H, Aiyelabegan HT, Negahdari B, Rajeian B, Zarghami N. Synthesis and characterization of chrysin-loaded PCL-PEG-PCL nanoparticle and its effect on breast cancer cell line. *Biomed Pharmacother.* (2016) 84:1915–22. doi: 10.1016/j.biopha.2016.10.095

36. Anari E, Akbarzadeh A, Zarghami N. Chrysin-loaded PLGA-PEG nanoparticles designed for enhanced effect on the breast cancer cell line. *Artif Cells Nanomed Biotechnol.* (2016) 44:1410–6. doi: 10.3109/21691401.2015.1029633

37. Rosen H, Abribat T. The rise and rise of drug delivery. *Nat Rev Drug Discov.* (2005) 4:381–5. doi: 10.1038/nrd1721

38. Danafar H. Applications of copolymeric nanoparticles in drug delivery systems. *Drug Res.* (2016) 66:506–19. doi: 10.1055/s-0042-109865

39. Danafar H, Rostamizadeh K, Davaran S, Hamidi M. Drug-conjugated PLA-PEG-PLA copolymers: a novel approach for controlled delivery of hydrophilic drugs by micelle formation. *Pharm Dev Technol.* (2017) 22:947–57. doi: 10.3109/10837450.2015.1125920

40. Duncan R, Ringsdorf H, Satchi-Fainaro R. Polymer therapeutics–polymers as drugs, drug and protein conjugates and gene delivery systems: past, present and future opportunities. *J Drug Target.* (2006) 14:337–41. doi: 10.1080/10611860600833856

41. Ting JM, Porter WW 3rd, Mecca JM, Bates FS, Reineke TM. Advances in polymer design for enhancing oral drug solubility and delivery. *Bioconjug Chem.* (2018) 29:939–52. doi: 10.1021/acs.bioconjchem.7b00646

42. Grossen P, Witzigmann D, Sieber S, Huwyler J. PEG-PCL-based nanomedicines: a biodegradable drug delivery system and its application. *J Control Release.* (2017) 260:46–60. doi: 10.1016/j.jconrel.2017.05.028

43. Zou T, Dembele F, Beugnet A, Sengmanivong L, de Marco A, Li MH. Nanobody-functionalized polymersomes. *J Control Release.* (2015) 213:e79–80. doi: 10.1016/j.jconrel.2015.05.132

44. Li R, Yan J, Xie L, Zhang Y, Gao J, Liu Q, et al. Facile optimization and evaluation of PEG-PCL block copolymeric nanoparticles for anticancer drug delivery using copolymer hybrids and histoculture drug response assays. *J Biomed Nanotechnol.* (2018) 14:321–30. doi: 10.1166/jbn.2018.2485

45. Sinha VR, Bansal K, Kaushik R, Kumria R, Trehan A. Poly-epsilon-caprolactone microspheres and nanospheres: an overview. *Int J Pharm.* (2004) 278:1–23. doi: 10.1016/j.ijpharm.2004.01.044

46. Cuong NV, Hsieh MF. Recent advances in pharmacokinetics of polymeric excipients used in nanosized anti-cancer drugs. *Curr Drug Metab.* (2009) 10:842–50. doi: 10.2174/138920009790274586

47. Otsuka H, Nagasaki Y, Kataoka K. PEGylated nanoparticles for biological and pharmaceutical applications. *Adv Drug Deliv Rev.* (2003) 55:403–19. doi: 10.1016/S0169-409X(02)00226-0

48. Zahr AS, Davis CA, Pishko MV. Macrophage uptake of core-shell nanoparticles surface modified with poly(ethylene glycol). *Langmuir.* (2006) 22:8178–85. doi: 10.1021/la060951b

49. Cuong NV, Hsieh MF, Chen YT, Liau I. Doxorubicin-loaded nanosized micelles of a star-shaped poly (epsilon-caprolactone) -polyphosphoester block co-polymer for treatment of human breast cancer. *J Biomater Sci Polym Ed.* (2011) 22:1409–26. doi: 10.1163/092050610X510533

50. Baidya D, Kushwaha J, Mahadik K, Patil S. Chrysin-loaded folate conjugated PF127-F68 mixed micelles with enhanced oral bioavailability and anticancer activity against human breast cancer cells. *Drug Dev Ind Pharm.* (2019) 45:852–60. doi: 10.1080/03639045.2019.1576726

51. Sarkar S, Nuttall RK, Liu S, Edwards DR, Yong VW. Tenascin-C stimulates glioma cell invasion through matrix metalloproteinase-12. *Cancer Res.* (2006) 66:11771–80. doi: 10.1158/0008-5472.CAN-05-0470

52. Sternlicht MD, Werb Z. How matrix metalloproteinases regulate cell behavior. *Annu Rev Cell Dev Biol.* (2001) 17:463–516. doi: 10.1146/annurev.cellbio.17.1.463

53. Juurikka K, Butler GS, Salo T, Nyberg P, Astrom P. The role of MMP8 in cancer: a systematic review. *Int J Mol Sci.* (2019) 20:4506. doi: 10.3390/ijms20184506

54. Cheng G, Fan X, Hao M, Wang J, Zhou X, Sun X. Higher levels of TIMP-1 expression are associated with a poor prognosis in triple-negative breast cancer. *Mol Cancer.* (2016) 15:30. doi: 10.1186/s12943-016-0515-5

55. Das K, Prasad R, Ansari SA, Roy A, Mukherjee A, Sen P. Matrix metalloproteinase-2: a key regulator in coagulation proteases mediated human breast cancer progression through autocrine signaling. *Biomed Pharmacother.* (2018) 105:395–406. doi: 10.1016/j.biopha.2018.05.155

56. Xia Y, Lian S, Khoi PN, Yoon HJ, Joo YE, Chay KO, et al. Chrysin inhibits tumor promoter-induced MMP-9 expression by blocking AP-1 via suppression of ERK and JNK pathways in gastric cancer cells. *PLoS ONE.* (2015) 10:e0124007. doi: 10.1371/journal.pone.0124007

57. Chen ZJ, Wei W, Jiang GM, Liu H, Wei WD, Yang X, et al. Activation of GPER suppresses epithelial mesenchymal transition of triple negative breast cancer cells via NF-kappaB signals. *Mol Oncol.* (2016) 10:775–88. doi: 10.1016/j.molonc.2016.01.002

58. Pandey DP, Lappano R, Albanito L, Madeo A, Maggiolini M, Picard D. Estrogenic GPR30 signalling induces proliferation and migration of breast cancer cells through CTGF. *EMBO J.* (2009) 28:523–32. doi: 10.1038/emboj.2008.304

59. Vivacqua A, Romeo E, De Marco P, De Francesco EM, Abonante S, Maggiolini M. GPER mediates the Egr-1 expression induced by 17β-estradiol and 4-hydroxitamoxifen in breast and endometrial cancer cells. *Breast Cancer Res Treat.* (2012) 133:1025–35. doi: 10.1007/s10549-011-1901-8

60. Wei T, Chen W, Wen L, Zhang J, Zhang Q, Yang J, et al. G protein-coupled estrogen receptor deficiency accelerates liver tumorigenesis by enhancing inflammation and fibrosis. *Cancer Lett.* (2016) 382:195–202. doi: 10.1016/j.canlet.2016.08.012

61. Chimento A, Sirianni R, Casaburi I, Zolea F, Rizza P, Avena P, et al. GPER agonist G-1 decreases adrenocortical carcinoma (ACC) cell growth *in vitro* and *in vivo*. *Oncotarget.* (2015) 6:19190–203. doi: 10.18632/oncotarget.4241

62. Medunjanin S, Schleithoff L, Fiegehenn C, Weinert S, Zuschratter W, Braun-Dullaeus RC. GSK-3beta controls NF-kappaB activity via IKKgamma/NEMO. *Sci Rep.* (2016) 6:38553. doi: 10.1038/srep38553